Optik 124 (2013) 538–543

Contents lists available at SciVerse ScienceDirect

Optik

journal homepage: www.elsevier.de/ijleo

Theoretical analysis and fabrication of tapered fiber

S.W. Harun[a,b,*], K.S. Lim[b], C.K. Tio[a], K. Dimyati[c], H. Ahmad[b]

[a] Department of Electrical Engineering, Faculty of Engineering, University of Malaya, 50603, Kuala Lumpur, Malaysia
[b] Photonics Research Center, Department of Physics, University of Malaya, 50603, Kuala Lumpur, Malaysia
[c] Department of Electrical and Electronic Engineering, Faculty of Engineering, National Defence University of Malaysia, Kem Sungai Besi, 57000 Kuala Lumpur, Malaysia

ARTICLE INFO

Article history:
Received 1 August 2011
Accepted 16 December 2011

Keywords:
Microfiber
Taper
Flame brushing technique
Adiabatic tapered fiber

ABSTRACT

Adiabaticity criteria and optimal shapes for tapered fiber are theoretically analyzed. In the analysis, it is discovered that a narrower taper waist can be achieved by using a small hot-zone length or increases the elongation distance. The tapered fiber fabrication based on flame brushing technique is then demonstrated using a homemade fiber tapering rig. The heat source comes from an oxy-butane torch with a flame width of 1 mm. Two stepper motors are incorporated in the rig to control the movement of the torch and translation stage. A biconical tapered fiber with a waist diameter as small as 400 nm can be achieved with the rig. To achieve low loss tapered fibers, the shape of the taper should be fabricated according to adiabaticity criteria, whereby the longer transition length is desirable. Tapered fibers with linear and decaying-exponential profiles have been successfully fabricated.

1. Introduction

Tapered fibers have recently attracted considerable interest as promising building blocks for a wide variety of photonic applications [1,2]. For instance, Tian et al. [3] reported a fast, highly sensitive and low-cost tapered optical fiber biosensor that enables the label-free detection of biomolecules. This is owing to their unique optical guidance properties that include a relatively low loss, strong evanescent fields, tight optical confinement, and controllable waveguide dispersion. They possess large refractive index contrast which is able to provide tight field confinement that makes tapered fibers particularly suitable for nonlinear optical applications [4]. Tapered fibers also offer an advantage of the ease of integration with conventional single mode fiber (SMF) as well as the access to the evanescent field provided by tapering since the light is guided by the boundary between the taper and the external environment. The external environment may be chosen to determine the number of modes supported by the waist, the bend tolerance and may provide a means of tuning through index of refraction or absorption control [5].

To produce high quality tapered fiber based devices, the tapered fibers used should have the following properties: high adiabaticity, uniform microfiber diameter, low surface roughness, and suitable microfiber diameter with large evanescent field. The tapered fiber diameter has a direct influence in the evanescent field and coupling coefficient of the tapered fiber coupling region in most devices. Basically, tapered fibers with thinner diameter have stronger evanescent field and thus yield higher coupling coefficient between two or more microfibers when they are put in a close contact with each other. Therefore, most tapered fiber based devices are assembled from tapered fibers with small diameter within 0.8–3 μm [6]. Besides, thin tapered fiber can be easily bent or coiled into smaller bending radius and thus smaller tapered fiber device can be produced. However, the difficulty in handling these tapered fibers increases with smaller diameter as thinner tapered fibers are very fragile and lossy.

Tapered fiber fabrications have been demonstrated by using a wide range of techniques: laser ablation [7], electron beam lithography [8], bottom-up methods such as vapor–liquid–solid techniques [9], and top–down techniques such as fiber pulling [10] or direct draw from bulk materials [11]. Among those methods, the flame heating technique has proven to be one of the most versatile, which can fabricate tapered fiber with good physical properties [12]. In this paper, tapered fiber fabrication is demonstrated using an automated fiber tapering rig based on flame brushing technique. The fabrication rig employs an oxy-butane torch, microcontroller and stepper motors. With the improved system, the problems of high insertion loss due to non-uniformity of tapered fiber can be reduced dramatically. Additionally, the system may realize fabrication of tapered fiber with waist diameter less than 1 μm or possibly in nano-range diameter. Adiabaticity criteria and optimal shapes for tapered fiber are also theoretically analyzed.

* Corresponding author at: University of Malaya, Dept. of Electrical Engineering, Faculty of Engineering, 50603 Kuala Lumpur, Malaysia.
E-mail address: swharun@um.edu.my (S.W. Harun).

0030-4026/$ – see front matter © 2012 Elsevier GmbH. All rights reserved.
doi:10.1016/j.ijleo.2011.12.054

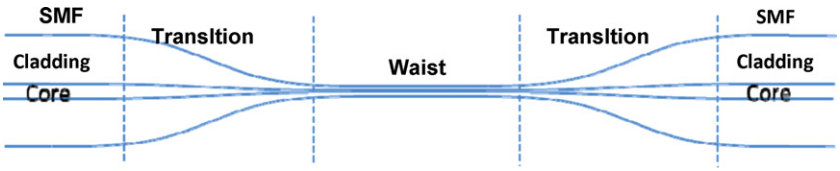

Fig. 1. Typical diameter profile of a tapered fiber.

2. Theoretical analysis of the tapered fiber

Tapered fiber is fabricated by stretching a heated conventional SMF to form a structure of reducing core diameter. As shown in Fig. 1, the smallest diameter part of the tapered fiber is called waist. Between the uniform un-stretched SMF and waist are the transition regions whose diameters of the cladding and core are decreasing from rated size of SMF down to the order micrometer or even nanometer. As the wave propagating through the transition regions, the field distribution varies with the change of core and cladding diameters along the way. Depend on the rate of diameter change, the energy transfer from the fundamental mode to a closest few higher order modes varies, which determines to the loss of the propagating wave power. The accumulation of this energy transfer along the tapered fiber may result to a substantial loss of throughput. This excessive loss can be minimized if the shape of the fabricated tapered fiber satisfies the adiabaticity criteria everywhere along the tapered fiber [13].

Fig. 2 gives an illustration of a tapered fiber with decreasing radius. z denotes the position along the tapered fiber. Theoretically, an adiabatic tapered fiber is based on the condition that the beat length between fundamental mode LP_{01} and second local mode is smaller than the local taper length-scale z_t.

$$z_b < z_t \tag{1}$$

Refer to illustration in Fig. 2, z_t is given by

$$z_t = \frac{\rho}{tan\Omega} \tag{2}$$

where $\rho = \rho(z)$ is the local core radius and $\Omega = \Omega(z)$ is the local taper angle. The beat length between two modes is expressed as

$$z_b = \frac{2\pi}{\beta_1 - \beta_2} \tag{3}$$

where $\beta_1 = \beta_1(r)$ and $\beta_2 = \beta_2(r)$ are the propagation constants of fundamental mode and second local mode respectively. From the above equations, Inequality of the tapered fiber can be derived to

$$\left|\frac{d\rho}{dz}\right| = \tan\Omega < \frac{\rho(\beta_1 - \beta_2)}{2\pi} \tag{4}$$

where $d\rho/dz$ is the rate of change of local core radius and its magnitude is equivalent to $\tan\Omega$. For the convenience of usage and analysis, the inequality of (4) can also be rewritten as a function of local cladding radius $r = r(z)$ as;

$$\left|\frac{dr}{dz}\right| < \frac{r(\beta_1 - \beta_2)}{2\pi} \tag{5}$$

Based on this condition, adiabatic tapered fiber can be acquired by tapering a fiber at a smaller reduction rate in diameter but this will result to a longer transition length. Considering practical limitations in the fabrication of fiber couplers or microfiber based devices, long tapered fiber may aggravate the difficulty in fabrication. For the purpose of miniaturization, short tapered fiber is preferable. To achieve balance between taper length and diameter reduction rate, a factor f is introduced to the Inequality function of (5) and yields

$$\frac{dr}{dz} < \frac{fr(\beta_1 - \beta_2)}{2\pi} \tag{6}$$

where the value of f can be chosen between 0 and 1. Optimal profile is achieved when $f = 1$. Practically, tapered fiber with negligibly loss can be achieved with $f = 0.5$ but the transition length of the tapered fiber is twice longer than that of the optimal tapered fiber.

When a glass element is heated, there is a small increment in the volume under the effect of thermal expansion. However, the change in volume is negligibly small not to mention that the volume expansion wears off very quickly once the heat is dissipated from the mass. It is reasonable to assume that the total volume of the heated fiber is conserved throughout the entire tapering process. Based on this explanation, when a heated glass fiber is stretched, the waist diameter of the fiber is reduced. The calculation of varying waist diameter and length of extension can be made based on the idea of 'conservation of volume' [13]. Birks and Li [13] have presented simple mathematical equations to describe the relationship between shapes of tapered fiber, elongation distance and hot-zone length. Any specific shape of tapered fiber can be controlled by manipulating these parameters in the tapering process. Fig. 3 provides schematic illustrations of heated fiber with reducing waist

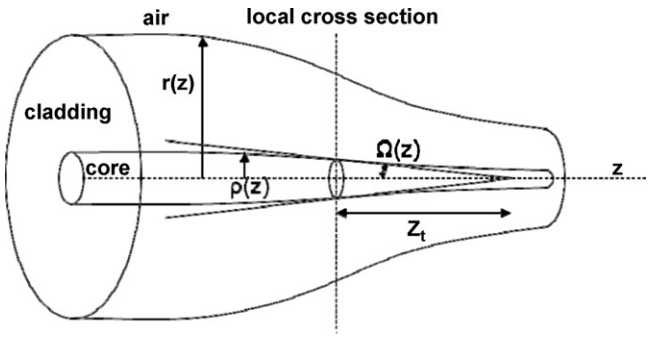

Fig. 2. Illustration of the taper transition.

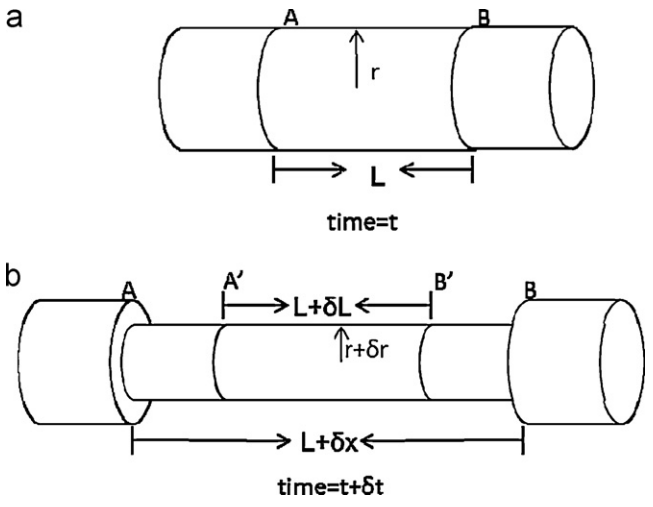

Fig. 3. The cylinder illustrates an SMF (a) before heating (b) a short while after heating, where the diameter of the SMF has been reduced when it is stretched.

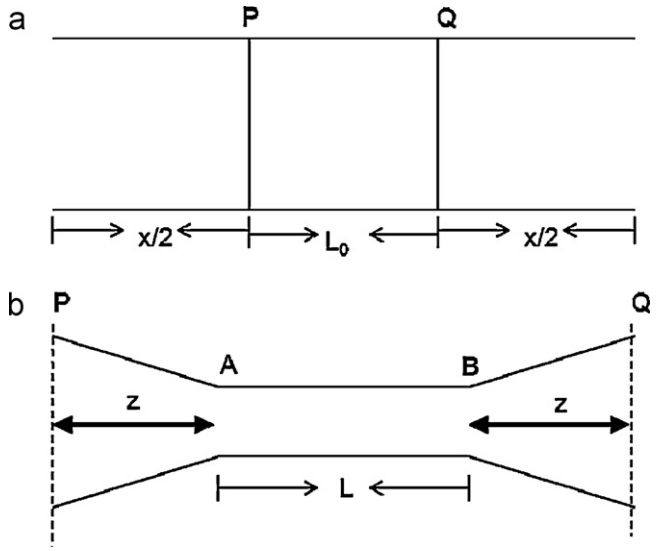

Fig. 4. Shape of a fiber (a) at the beginning ($t = 0$) (b) after tapering (time = t).

diameter during the elongation process. At time t, the heated fiber bounded between cross sections A and B has a length equivalent to the hot-zone length L and the waist diameter is denoted by r. After a short interval of time δt, the heated fiber is stretched and the length is extended to $L + \delta x$. The diameter of heated fiber becomes $r + \delta r$ where δr denotes the change in the waist radius. The volume of the stretched fiber at time $t + \delta t$ should be the same with the volume at time t

$$\pi(r + \delta r)^2(L + \delta x) = \pi r^2 L \tag{7}$$

After some algebraic manipulations, a differential equation can be derived from Eq. (7), which is given as;

$$\frac{dr}{dx} = \frac{r}{2L} \tag{8}$$

The function of radius profile is given by the integral

$$r(x) = r_0 \exp\left(-\frac{1}{2}\int \frac{dx}{L}\right) \tag{9}$$

where r_0 denotes the initial radius of the fiber. To relate the varying hot-zone length L with the elongation distance x during the tapering process, L can be replaced with any function of x. Linear function

$$L(x) = L_0 + \alpha x \tag{10}$$

makes a convenient function for the integral in Eq. (9).

$$r(x) = r_0 \exp\left(-\frac{1}{2}\int \frac{dx}{L_0 + \alpha x}\right) \tag{11}$$

$$r(x) = r_0\left(1 + \frac{\alpha x}{L_0}\right)^{-1/2\alpha} \tag{12}$$

To relate elongation distance x with the position on taper transition z, another equation is derived by referring to model in Fig. 4. L_0 in Fig. 4(a) denotes the initial hot-zone length bounded by cross-sections P and Q of the fiber while x denotes the elongation distance. Consider the heated fiber is elongated to form a biconical shape. The elongation results to two identical extensions of taper on both sides of the hot zone, each length of $x/2$. After tapering for time = t, P and Q have been elongated for an extension of x and the length of the taper waist is L. Based on the above description, it is easy to obtain the following equation

$$2z + L = x + L_0 \tag{13}$$

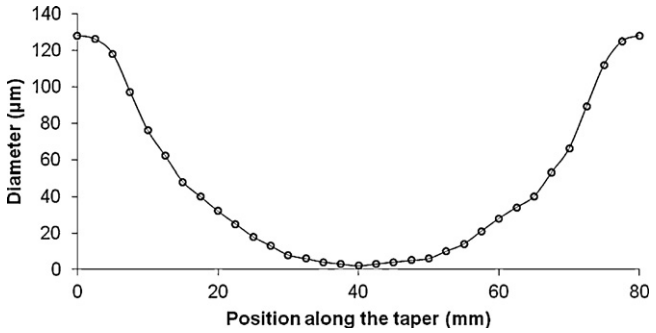

Fig. 5. A tapered fiber with decaying-exponential profile fabricated using a constant hot-zone $L_0 = 10$ mm.

where $L = L(x)$. Substituting Eq. (13) to Eq. (12) yields

$$r(z) = r_0\left(1 + \frac{2\alpha z}{(1-\alpha)L_0}\right)^{-1/2\alpha} \tag{14}$$

where α is the constant that varies from −1 to 1.

By manipulating the value of α, several shapes of tapered fiber can be produced such as reciprocal curve, decaying-exponential, linear and concave curve. Several examples of calculated taper shape based on different values of α can be found in the literature of [13]. Fig. 5 shows a tapered fiber profile fabricated using a constant hot-zone $L_0 = 10$ mm. As shown in the figure, the tapered fiber has a decaying-exponential profile and thus the fabrication requires a constant hot-zone length ($\alpha = 0$). From the theoretical model presented above, the function for the decaying-exponential profile is given by

$$r(z) = r_o e^{-z/L_0} \tag{15}$$

Based on this profile function, narrower taper waist can be achieved by using a small hot-zone length in the fabrication or drawing the taper for a longer elongation distance. Tapered fiber with short transition length can achieved from reciprocal curve profile based on positive value of α particularly with $\alpha = 0.5$.

Linear taper profile can be produced using $\alpha = -0.5$ as shown in Fig. 6. Curve profile (a) in Fig. 6 shows a typical example of linear taper profile where its smallest waist point is at the center of the tapered fiber. By doing some simple modification on the tapering process, the smallest waist point can be shifted away from the center to one side of the tapered fiber as shown by profiles (b and c) in the same figure. These profiles are found useful in the fabrication of wideband chirped fiber Bragg gratings, in which the grating is written on the transitions of the tapered fiber. Long linear shape tapers

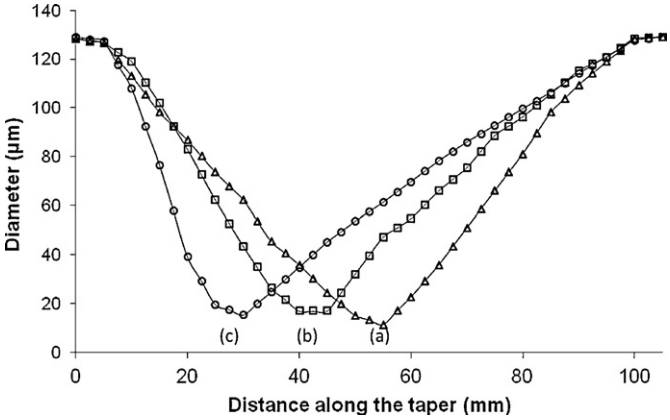

Fig. 6. Three linear taper profiles where the smallest waist point is located at different positions on the tapered fiber. Profile (a) has its smallest waist point at the center of the tapered fiber.

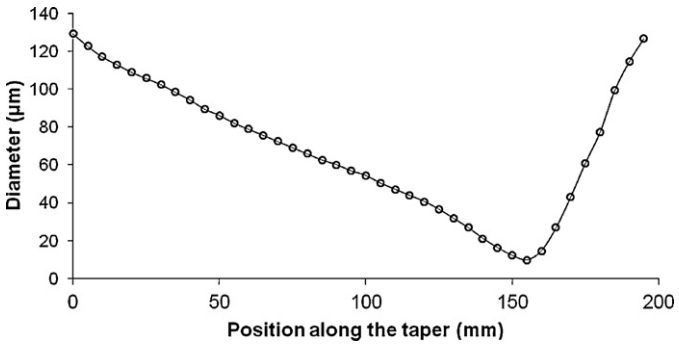

Fig. 7. The diameter of tapered fiber is linearly decreasing from ~128 μm to ~10 μm along the 15 cm transition.

make good candidates for the fabrication of such devices [14]. On the other hand, linear profile tapers can be used for optical tweezing because of its capability to converge the optical wave to a high intensity at the taper tip [15]. Microscopic objects are attracted to the high intensity field driven by the large gradient force at the taper tip. Fig. 7 gives a good example of such tapered fiber with 15 cm linear taper profile. It was produced by using a long initial hot zone length L_0 = 7 cm and long elongation distance.

2.1. Tapered fiber fabrication

Fig. 8 shows the picture of the fiber tapering rig assembled in the laboratory. It mainly comprises of two fiber holders on a linear translation stage, a sliding stage, an oxy-butane burner which is fixed on the sliding stage, two stepper motors and the motor controller board. The oxygen gas and butane gas of the oxy-butane torch are supplied from separate gas cylinders. The mixing of both gases takes place in the torch chamber and the mixture is supplied to a ~1 mm sized pin-point flame at the torch tip. Fig. 9 shows the torch flames of different oxygen supply pressure. The flame size is the largest without the oxygen as shown in Fig. 9(a). In the experiment, both oxygen and butane gas pressures are regulated at ~5 psi each as shown in Fig. 9(b). The convective air flow from the flame is kept at an acceptably low level and the flame temperature is high enough to heat and soften the silica fiber. However, the flame temperature can be further increased by supplying higher pressure of oxygen to the torch as shown in Fig. 9(c), but the flame may go out easily due to fast depletion of fuel gas and the fast convective air flow could result in bending the heated SMF and inducing high insertion loss in the tapered fiber.

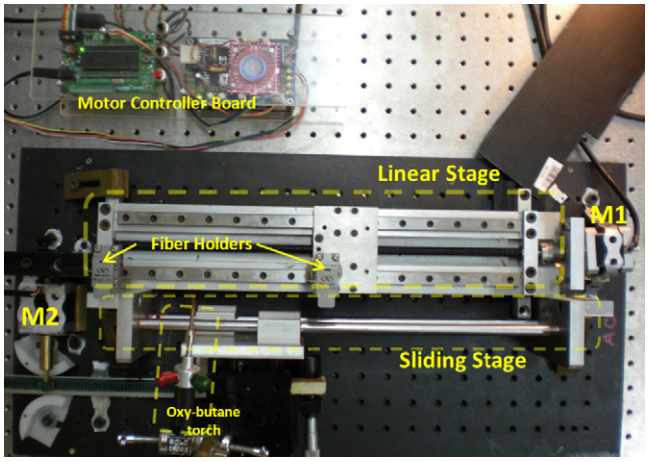

Fig. 8. Picture of the fiber tapering Rig assembled in the laboratory. M1 and M2 are the stepper motors of the linear stage and sliding stage respectively.

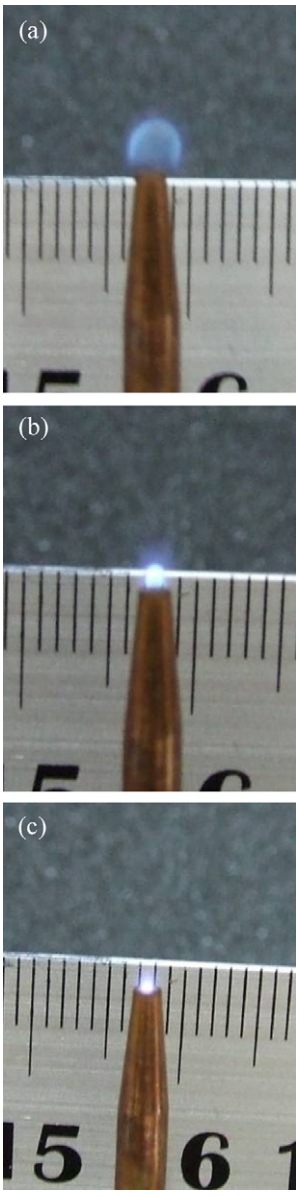

Fig. 9. Torch flames at different oxygen supply pressure (a) none (b) equivalent pressure with fuel gas pressure (c) high oxygen.

In controlling the linear stage and sliding stage traveling speed and position, two high precision stepper motors (LINIX Stepping Motor, Product Code: 42BYGHD-444) with a resolution of 1.8°/step are deployed. Translating the rotation resolution to the linear stage, the linear stage travels at a resolution of 2.5 μm/step and it can reach a maximum speed of 59.6 mm/s. The linear stage is used for stretching the heated SMF. To fabricate smooth and low loss tapered fibers, the linear stage is often traveling at a very low velocity (0.8–1.8 mm/s). In flame-brushing a tapered fiber, the oxy-butane torch is required to travel at higher speed than the linear stage to provide a uniform heat a long tapered fiber. In order to achieve that, the torch is mounted on a custom-made sliding stage that can travel at a very high speed in a linear direction. In this work, the sliding stage is programmed to travel at the moderate speed from 10 to 40 mm/s with a resolution of 317.5 μm/step.

The motor control system of the rig plays the most important part in controlling the stages position, speed and moving direction. The quality of the tapered fiber lies on the routine of the torch movement and linear stage pulling length and speed. With

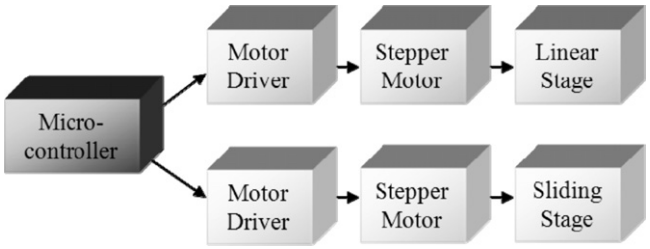

Fig. 10. System diagram of the motor control in the fiber tapering rig.

the incorporation of microcontroller in the system, the tapering routine can be written into a code and programmed into the microcontroller. With that, any microfibers with specific diameter and length can be fabricated accurately and reproduced based on the same tapering routine. Fig. 10 shows the system diagram of the motor control system of the rig. The microcontroller sits at the top of the motor control system hierarchy, coordinating and controlling two different stepper motors. Each stepper motor is equipped with a motor driver and both combinations of motor driver and stepper motor are assigned to the linear stage and sliding stage respectively. Microchip PIC18F4520 is used as microcontroller in the system. The tapering routine is written in C language by using MPLAB IDE vs8.53. The code is then converted into a format that can be programmed into the microcontroller using PICkit 2 Development Programmer.

Fig. 11 shows the schematic experimental setup to fabricate a tapered fiber using a flame brushing technique. As shown in Fig. 11, coating length of several cm is removed from the SMF prior to the fabrication of tapered fiber. Then the SMF is placed horizontally on the translation stage and held by two fiber holders. During the tapering, the torch moves and heats along the uncoated segment of fiber while the fiber is being stretched. The moving torch provides a uniform heat to the fiber so that the tapered fiber is produced with good uniformity along the heat region. To monitor the transmission spectrum of the microfiber during the fabrication, amplified spontaneous emission (ASE) source from an erbium-doped fiber amplifier (EDFA) is injected into one end of the SMF while the other end is connected to the optical spectrum analyzer (OSA). Fig. 12(a) shows diameter variation of the biconical tapered fiber fabricated using the fiber tapering rig and Fig. 12(b) shows the optical microscope image of waist of the tapered fiber, 1.7 μm in diameter. With proper tapering parameters, the taper waist diameter can narrowed down to ~400 nm as shown in Fig. 12(c).

Adiabaticity is one of the important criteria in fabricating good quality tapered fibers. It is commonly known that some tapered fibers suffer loss of power due to the loss of power when the fundamental mode couples to the higher order modes. Some fraction of power from higher order modes that survives propagating through the tapered fiber may recombine and interfere with

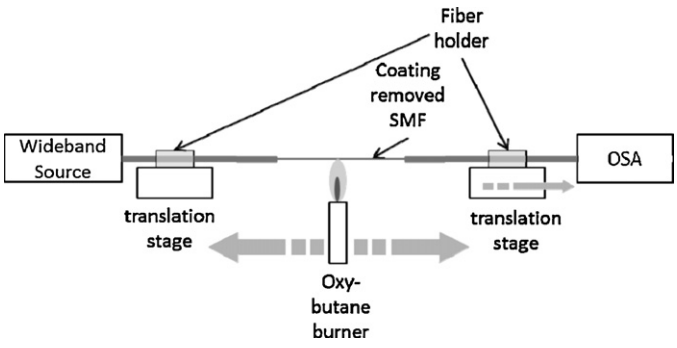

Fig. 11. Schematic illustration of flame brushing technique.

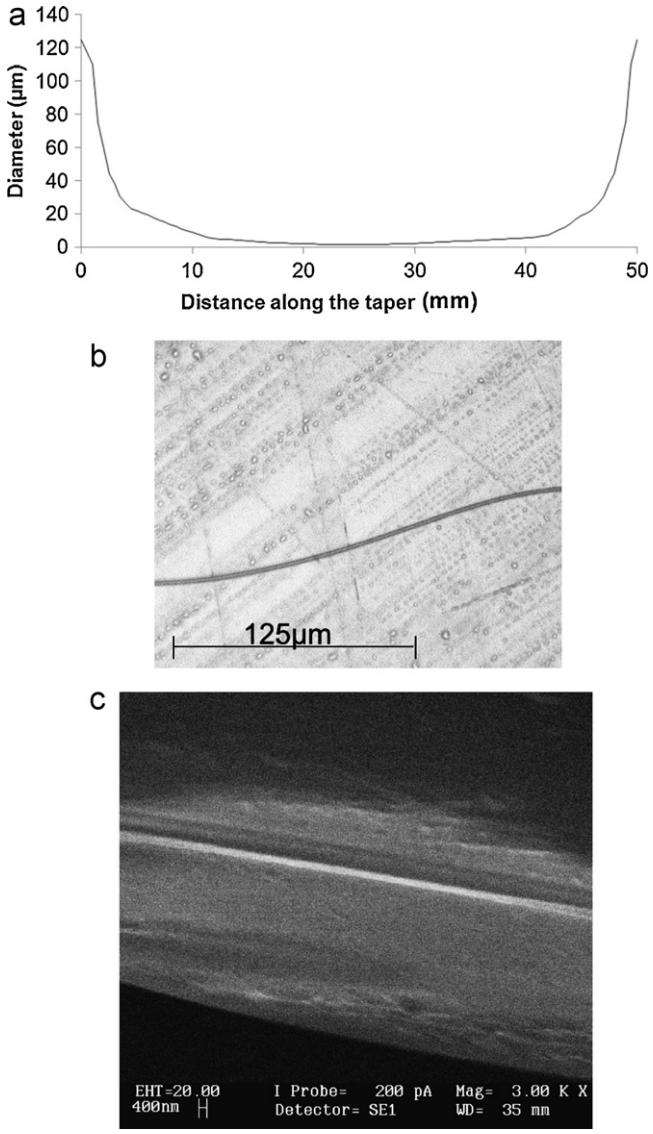

Fig. 12. Characteristic of the fabricated tapered fiber (a) the diameter variation of a biconical tapered fiber fabricated in the laboratory (b) optical microscope image of taper waist, 1.7 μm in diameter (c) SEM image of a 400 nm waist diameter tapered fiber.

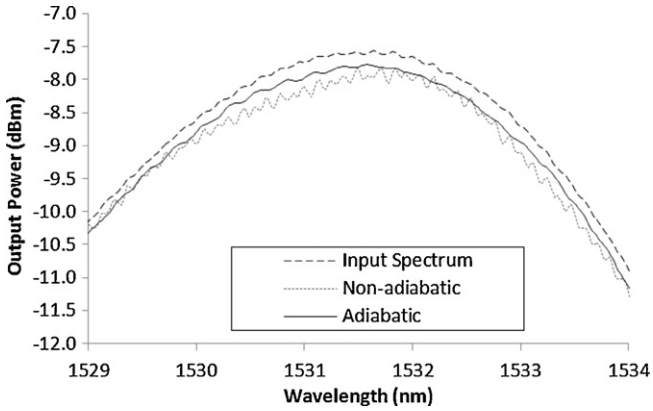

Fig. 13. Output spectra from a microfiber with 10 cm long and ~3 μm waist diameter. Input spectrum from EDFA (dashed), adiabatic taper (solid) and non-adiabatic taper (dotted).

fundamental mode. This phenomenon can be seen as interference between fundamental mode HE_{11} and its closest higher order mode HE_{12}. This results to a transmission spectrum with irregular fringes as shown by the dotted graph in Fig. 13 and the excessive loss of the tapered fiber is ~0.6 dB [15,16]. This tapered fiber is not suitable to be used in the ensuing fabrication of microfiber devices. The solid curve in the same figure shows the transmission of a low loss tapered fiber with approximately more than 4 mm transition length and the insertion loss lower than 0.3 dB. Some analysis suggests that the coupling from fundamental mode to higher order modes can be minimized by optimizing shape of the tapers. In most practice, adiabaticity can be easily achieved by using sufficiently slow diameter reduction rates when drawing tapered fibers or in other words manufacture tapered fibers with sufficiently long taper transition length.

3. Conclusion

Tapered fiber is fabricated by stretching a heated SMF using a flame brushing technique. Adiabaticity criteria and optimal shapes for tapered fiber are theoretically analyzed to assist in the fabrication. It is discovered that a narrower taper waist can be achieved by using a small hot-zone length or increases the elongation distance. The fabrication rig employs an oxy-butane torch with a flame width of 1 mm as the heat source in conjunction with two stepper motors to control the movement of the torch and translation stage. A biconical tapered fiber with a waist diameter as small as 400 nm can be achieved using the fabrication technique. It is found that the shape of the taper should follow the adiabaticity criteria and has a longer transition length to achieve low loss characteristic. Tapered fibers with linear and decaying-exponential profiles have been successfully fabricated.

References

[1] K.S. Lim, S.W. Harun, S.S.A. Damanhuri, A.A. Jasim, C.K. Tio, H. Ahmad, Current sensor based on microfiber knot resonator, Sens. Actuators A 167 (2011) 60–62.
[2] S.W. Harun, K.S. Lim, A.A. Jasim, H. Ahmad, Dual wavelength erbium-doped fiber laser using a tapered fiber, J. Mod. Opt. 57 (2011) 2111–2113.
[3] Y. Tian, W. Wang, N. Wu, X. Zou, X. Wang, Tapered optical fiber sensor for label-free detection of biomolecules, Sensors 11 (2011) 3780–3790.
[4] G. Vienne, Y. Li, L. Tong, Ph. Grelu, Observation of a nonlinear microfiber resonator, Opt. Lett. 33 (2008) 1500–1502.
[5] G. Brambilla, F. Xu, X. Feng, Fabrication of optical fibre nanowires and their optical and mechanical characterization, Electron. Lett. 42 (2006) 517.
[6] M. Sumetsky, Y. Dulashko, J.M. Fini, A. Hale, D.J. DiGiovanni, The microfiber loop resonator: theory, experiment, and application, J. Lightwave Technol. 24 (1) (2006) 242–250.
[7] A.M. Morales, C.M. Lieber, A laser ablation method for the synthesis of crystalline semiconductor nanowires, Science 279 (January (5348)) (1998) 208–211.
[8] J. Chen, M.A. Reed, A.M. Rawlett, J.M. Tour, Large on–off ratios and negative differential resistance in a molecular electronic device, Science 286 (5444) (1999) 1550–1552.
[9] J. Westwater, D.P. Gosain, S. Tomiya, S. Usui, H. Ruda, Growth of silicon nanowires via gold/silane vapor–liquid–solid reaction, J. Vac. Sci. Technol. B: Microelectron. Nanometer Struct. 15 (3) (1997) 554–557.
[10] A.M. Clohessy, N. Healy, D.F. Murphy, C.D. Hussey, Short low-loss nanowire tapers on singlemode fibres, Electron. Lett. 41 (17) (2005) 954–955.
[11] X. Xing, Y. Wang, B. Li, Nanofibers drawing and nanodevices assembly in poly(trimethylene terephthalate), Opt. Express 16 (14) (2008) 10815–10822.
[12] S.W. Harun, K. Lim, A. Jasim, H. Ahmad, Fabrication of tapered fiber based ring resonator, Laser Phys. 20 (7) (2010) 1629–1631.
[13] T.A. Birks, Y.W. Li, The shape of fiber tapers, J. Lightwave Technol. 10 (4) (1992) 432–438.
[14] O. Frazão, et al., Chirped Bragg grating fabricated in fused fibre taper for strain–temperature discrimination, Meas. Sci. Technol. 16 (4) (2005) 984.
[15] Z. Liu, C. Guo, J. Yang, L. Yuan, Tapered fiber optical tweezers for microscopic particle trapping: fabrication and application, Opt. Express 14 (25) (2006) 12510–12516.
[16] L. Ding, C. Belacel, S. Ducci, G. Leo, I. Favero, Ultralow loss single-mode silica tapers manufactured by a microheater, Appl. Opt. 49 (13) (2010) 2441–2445.